

A Simultaneous Optical and X-ray Variability Study of the Orion Nebula Cluster. II. A Common Origin in Magnetic Activity

Keivan G. Stassun¹, M. van den Berg², Eric Feigelson³

ABSTRACT

We present a statistical analysis of simultaneous optical and X-ray light curves, spanning 600 ks, for 814 pre-main-sequence (PMS) stars in the Orion Nebula Cluster. The aim of this study is to establish the relationship, if any, between the sites of optical and X-ray variability, and thereby to elucidate the origins of X-ray production in PMS stars. In a previous paper we showed that optical and X-ray variability in PMS stars are very rarely time-correlated. Here, using time-averaged variability indicators to examine the joint occurrences of optical and X-ray variability, we confirm that the two forms of variability are not directly causally related. However, a strong and highly statistically significant correlation is found between optical variability and X-ray luminosity. As this correlation is found to be independent of accretion activity, we argue that X-ray production in PMS stars must instead be intimately connected with the presence and strength of optically variable, magnetically active surface regions (i.e. spots) on these stars. Moreover, because X-ray variability and optical variability are rarely time-correlated, we conclude that the sites of X-ray production are not exclusively co-spatial with these regions. We argue that solar-analog coronae, heated by topologically complex fields, can explain these findings.

Subject headings: open clusters and associations: individual (Orion Nebula Cluster)—stars: flare—stars: magnetic fields—stars: spots—stars: pre-main-sequence—X-rays: stars

1. Introduction

While it is now well established that low-mass pre-main-sequence (PMS) stars typically have X-ray luminosities 2–4 orders of magnitude higher than that of the present-day Sun (e.g. Preibisch et al. 2005), fundamental questions remain as to how these X-rays are actually produced. Observations of X-ray flares in these stars indicate solar-analog magnetic reconnection events, but the absence of an obvious main-sequence-like rotation-activity relation in PMS stars has so far confounded attempts to ascribe PMS X-ray production directly to dynamo-generated fields (Flaccomio et al. 2003; Feigelson et al. 2003; Stassun et al. 2004; Rebull et al. 2006). Accretion has also been implicated as a possible driver of PMS X-ray production, but no consensus has emerged on this point as yet (e.g. Kastner et al. 2002; Stelzer & Schmitt 2004; Stassun et al. 2004). Indeed, there is evidence that accretion may act to inhibit X-ray production instead of enhance it (e.g. Flaccomio et al. 2003; Preibisch et al. 2005). These issues are reviewed more fully in Feigelson et al. (2006).

¹Department of Physics & Astronomy, Vanderbilt University, Nashville, TN 37235; keivan.stassun@vanderbilt.edu

²Harvard-Smithsonian Center for Astrophysics, 60 Garden St., Cambridge, MA 02138

³Department of Astronomy & Astrophysics, Penn State University, University Park, PA 16802

X-rays from PMS stars are interesting not only because of the mystery surrounding their origins. If X-rays trace magnetic activity in young stars as they do in main sequence stars, then X-rays can provide important clues to a variety of star-formation questions involving stellar magnetic fields—the evolution of stellar angular momentum via magnetized winds and magnetic coupling to circumstellar disks, for example. X-rays may also be central players in the physics of molecular clouds and protoplanetary disks, driving the photoionization of circumstellar material (e.g. Glassgold, Feigelson, & Montmerle 2000). Thus, understanding the physics of X-ray production in PMS stars may ultimately prove central to our understanding of star- and planet-formation (Feigelson et al. 2006).

To make progress in understanding *how* PMS X-rays are made, it would be valuable to have constraints on *where* the X-rays are coming from. A key limitation in this regard has been the lack of simultaneous, independent measures of X-ray production and of other forms of activity, such as optical variability. So motivated, we have undertaken an extensive variability study of the Orion Nebula Cluster (ONC) combining a nearly continuous, 13-d *Chandra* observation with simultaneous, multi-wavelength, time-series photometry in the visible. The resulting database of simultaneous X-ray and optical light curves for some 800 members of the ONC represents, by a factor of hundreds, the largest attempt to date to study the relationship between X-ray and optical variability in PMS stars (Stassun et al. 2006, hereinafter Paper I).

In Paper I, we used this database to search for time-correlated variability in our simultaneous optical and X-ray light curves with the goal of establishing the frequency with which X-ray and optical variations are co-temporal, and to thereby constrain the extent to which the sources of X-ray and optical variability may be co-spatial or otherwise causally linked. For example, if X-rays are produced near accretion shocks on classical T Tauri stars (CTTSs; actively accreting PMS stars), then one might expect that changes in the strength of these shocks will induce changes in the strength of the X-ray emission, and that X-ray and optical variability might therefore be correlated in time. Similarly, if X-rays originate in coronal structures associated with magnetically active surface regions on these stars (i.e. dark spots), we might then expect that optical and X-ray variability would be anti-correlated in time. However, we found that such behavior almost never occurs. Indeed, except for a single possible case of “white light” flare emission, simultaneous X-ray/optical variations were not clearly seen in any of the 800+ stars observed. The upper limit on the incidence of time-correlated optical/X-ray variability in our sample is at most $\sim 5\%$; that is, at least $\sim 95\%$ of the stars in our sample exhibit no evidence for time-correlated optical and X-ray variability (Paper I). The implication is that the sites of optical and X-ray variability in PMS stars are not—in the vast majority of cases—instantaneously one and the same. Similar findings have now also been reported from a simultaneous optical/X-ray monitoring survey of Taurus by Audard et al. (2007).

Whereas these findings rule out the simple interpretation of the X-ray and optical variability both dominated by one site of emission, in this companion paper we examine the possibility of a more general relationship between optical and X-ray variability by investigating *time-averaged* optical and X-ray variability indicators (e.g. variability amplitudes) and possible correlations therein. After reviewing the salient contents of our simultaneous optical/X-ray variability database, and the time-averaged variability indicators that we use in our analysis (§2), in §3 we perform a multivariate correlation analysis of these indicators with one another and with other stellar properties related to energy production (accretion signatures, bolometric luminosity, X-ray luminosity). We find that time-averaged optical and X-ray variability are not well correlated with one another, implying that they are not causally related. Importantly, however, we do find optical variability to be strongly correlated with X-ray *luminosity*, and that this correlation exists regardless of whether the stars in question are actively accreting (CTTSs) or non-accreting (weak-lined T Tauri stars; WTTSs).

We discuss in §4 the implications of these results. We argue that accretion is not in general a significant contributor to the production of X-rays in CTTSs, and that PMS X-ray production overall is more intimately related to the presence of magnetically active surface regions (i.e. spots), as traced by optical variability, in both CTTSs and WTTSs. At the same time, the lack of time-correlated optical and X-ray variability in the overwhelming majority of our sample (Paper I) indicates that the X-rays are not produced in magnetically active surface regions alone. We summarize our conclusions in §5.

2. The COUP synoptic X-ray and optical database

A complete description of our database of simultaneous X-ray and optical light curves is provided in Paper I. Briefly, the database comprises 814 PMS members of the ONC within a $17' \times 17'$ region centered on the Trapezium observed by ACIS onboard *Chandra* for 13.2 d. These stars were simultaneously observed at *BVRI* wavelengths by small telescopes on the ground during the last 7 d of the *Chandra* observation, with a cadence of $\sim 1 \text{ hr}^{-1}$.

For each star, the database also includes the star’s X-ray luminosity, L_X (Getman et al. 2005), and a compilation of other physical parameters from photometric and spectroscopic catalogs already in the literature, including bolometric luminosity, L_{bol} (Hillenbrand 1997), and the equivalent width (EW) of the Ca II infrared triplet from Hillenbrand et al. (1998), a measure of mass accretion rate. As in previous studies (e.g. Flaccomio et al. 2003; Stassun et al. 2004; Preibisch et al. 2005, Paper I), we take the “accretors” to be those stars with Ca II strongly in emission, i.e., $\text{EW} \leq -1 \text{ \AA}$, and “non-accretors” to be those with Ca II clearly in absorption, i.e., $\text{EW} \geq 1 \text{ \AA}$. Of the 493 stars in our study sample with Ca II measurements, 151 stars are accretors and 145 stars are non-accretors, as defined here (the remainder show indeterminate values close to 0 \AA)¹.

The 814 stars in our database span a very large range of apparent magnitudes and colors, with $7.3 < I < 18.4$ and $-0.1 < (V - I) < 5.7$, and a correspondingly large range of spectral types and extinctions, $\text{B3} < \text{SpTy} < \text{M7}$ and $0.0 < A_V < 10.8$ (Hillenbrand 1997). This sample is thus representative of the underlying ONC population; only the very massive, heavily obscured, and sub-stellar populations are excluded.

These stars exhibit a large variety of behaviors in their optical and X-ray variability. Figs. 1–6 in Paper I show the optical and X-ray light curves for a selection of objects as a representative visual summary of the range and types of variability observed. Below we describe the statistical indicators that we use to quantify the time-averaged X-ray and optical variability.

¹As a caveat, we note that $\text{EW}[\text{Ca II}]$ is an imperfect indicator of accretion. As shown by Sicilia-Aguilar et al. (2005), some PMS stars with clear accretion signatures in $\text{H}\alpha$ do not manifest this accretion activity in Ca II. It is therefore possible or even likely that some low-level accretors will go undetected in Ca II. The criterion that we adopt for identifying the presence of accretion is thus in practice a conservative one; stars with $\text{EW}[\text{Ca II}] \leq -1 \text{ \AA}$ and $\text{EW}[\text{Ca II}] \geq 1 \text{ \AA}$ are securely identified as accretors and non-accretors, while some stars with indeterminate values close to 0 \AA may be weakly accreting objects that will go unidentified as such.

2.1. Time-averaged variability indicators

2.1.1. X-ray variability

The COUP database provides two measures of X-ray variability in the detected X-ray sources. These are discussed in detail by Getman et al. (2005).

The first measure is a standard one-sided Kolmogorov-Smirnoff (KS) test, which tests the null hypothesis that the photon arrival times are distributed uniformly in time. The KS test thus gives the probability that the source’s X-ray flux is consistent with being non-variable (i.e. constant). We take sources with KS test probabilities of less than 0.001 as being definitively X-ray variable, the expected number of false positives in our sample then being less than 1. Of the 814 sources in our study sample, 556 (68%) are X-ray variable at greater than 99.9% confidence by this definition.

The second measure of time-averaged X-ray variability is a Bayesian Block (BB) analysis (Scargle 1998), which segments each light curve into the maximum number of time blocks such that the differences in the mean flux levels of the blocks are statistically significant. The BB analysis thus yields a robust measure of the maximum and minimum flux levels in the source’s X-ray light curve (BB_{\max} and BB_{\min} , respectively). In our analysis, we use the ratio BB_{\max}/BB_{\min} to quantify the magnitude of variability in the X-ray light curves of stars in our sample. The X-ray variables in our database have a range of amplitudes $0.12 < \log(BB_{\max}/BB_{\min}) < 2.89$ (see Fig. 1). The KS and BB measures of time-averaged X-ray variability for the stars in our study sample are reported in Table 1.

2.1.2. Optical variability

To characterize the time-averaged optical variability of the stars in our sample we use the J statistic described by Stetson (1996). Similar to the standard χ^2 statistic, the J statistic measures the residuals of the data about the weighted mean level of the light curve, and compares those residuals to the measurement uncertainties. However, unlike a standard χ^2 analysis, the Stetson index simultaneously considers the measurements from light curves in all available photometric bands of a given source. This is done by pair-wise matching the data points in time and comparing the signs of the matched residuals.

$$J \equiv \frac{\sum_{i=1}^p w_i \operatorname{sgn}(P_i) \sqrt{|P_i|}}{\sum_{i=1}^p w_i}$$

where p is the number of pairs of observations of the star, $P_i = \delta_{j(i)}\delta_{k(i)}$ is the product of the normalized residuals of the paired measurements, and w_i is the statistical weight assigned to each pair (see Stetson 1996, for details on weights). The normalized residual of measurement i in passband j is given by

$$\delta_{j(i)} = \sqrt{\frac{n}{n-1}} \frac{m_i - \overline{m}}{\sigma_i}$$

where n is the number of measurements used to determine the mean magnitude \overline{m} , and σ_i is the photometric uncertainty in measurement m_i .

The J statistic is more robust than χ^2 against outliers. As an example, consider a non-variable star with simultaneous light curves in three passbands, and consider the case where a cosmic ray hit appears

as a discrepantly high data point in one of these three light curves. This one outlier will increase the value of the χ^2 statistic for that light curve, making it appear variable in one passband but not in the others. In contrast, this outlier will tend to decrease the value of the J statistic. Following the procedure of Stetson (1996) to make the J statistic even more robust, we compute the J statistic iteratively, adjusting the weights of individual data points and re-computing the weighted mean of each light curve between successive iterations, thereby minimizing the influence of strong outliers on the J statistic.

To calculate J in practice, the light curves must be binned in time, which requires a choice of binning timescale. This binning is not in the sense of combining adjacent data points; rather, time bins are defined to determine which data points from the multiple light curves are associated with one another in the pair-wise matching discussed above. Given the typical sampling and cadence of the optical light curves (see Paper I), we adopt time bins of 1 hr.

Values of J for the stars in our study sample are reported in Table 1. For each star we also report in Table 1 the measures of time-averaged X-ray variability and of accretion discussed above. The distribution of J for our study sample is shown in Fig. 1. From this distribution, we can empirically choose a threshold of J , above which we may be confident that the optical light curves manifest true variability. True variable stars will show positive values of J , the magnitude of which is related to the amplitude of the variability. In comparison, non-variable stars will produce a narrow distribution of J centered about zero, with equal probability for being positive or negative. This narrow distribution of values about zero represents the probability distribution of J arising from small, chance correlations in the optical light curves, and we may thus use the most negative value of J as a conservative estimate of the most positive value of J that will result from such chance correlations.

The distribution of J in our sample (Fig. 1) shows a maximal negative value of $J = -1.50$. This value occurs once in our sample of 814 stars, and we may therefore expect that a value of $J > 1.50$ will occur by chance with a probability of $1/814 \approx 0.001$, which is the same as the conservative criterion we have adopted for identifying variability in the X-ray light curves.

With this threshold, 358/814 (44%) of the stars are optically variable, with a range $1.5 < J \leq 45.5$. The optical and X-ray light curves for a selection of sources with J spanning this range are shown in Figs. 1–6 in Paper I. In general, larger values of J imply greater variability. The threshold of $J > 1.50$ that we adopt for identifying truly variable objects corresponds roughly to peak-to-peak variability of ~ 0.05 mag (typical photometric errors are 0.01–0.02 mag; Paper I), though for any particular source the peak-to-peak variability is different at the different wavelengths (generally larger at shorter wavelengths due to the increased temperature contrast). Thus, sources identified as “non-variable” in fact represent upper limits of peak-to-peak variability less than $\sim 5\%$. At the other extreme, objects with the largest J values show peak-to-peak variability in the V band of $\gtrsim 2$ mag. With this range of variability amplitudes, the time-averaged optical variability of our sample is typical of what has been observed before in optical variability studies of TTSs (e.g. Herbst et al. 1994).

3. Results: Statistical analysis of time-averaged variability indicators

Here we report the results of a statistical analysis of these variability indicators, with the goal of determining their relationships with one another and with other stellar parameters. We present three levels of analysis in order of increasing sophistication (§§3.1–3.3) with a concise summary in §3.4. All statistical

analyses reported here were performed with the R software² package.

3.1. Relation of optical and X-ray variability to accretion

One of the aims of our study is to determine whether accretion may be a significant contributor to the production of X-rays in PMS stars. We have already seen in Paper I that there is no evidence in the form of time-correlated X-ray and optical variability for such a connection, implying that any causal relationship between accretion and X-ray production must be indirect. Here we consider whether the presence of active accretion manifests itself in the time-averaged variability of our sample.

Applying a Student’s t test to the distributions of X-ray variability (BB_{\max}/BB_{\min}) for the accretors and non-accretors, we find a probability of 38% that these two groups have similar mean values of BB_{\max}/BB_{\min} . That is, there is not a statistically significant difference in the level of X-ray variability among the accretors as compared to the non-accretors.

In contrast, accretion does manifest itself in the optical variability of these stars. A t test applied to the same accretor and non-accretor samples confirms, at the 99% confidence level, that accretors exhibit higher average levels of optical variability (J) than the non-accretors. This is as expected, since optical variability in CTTSs is believed to be driven in part by accretion. This result is also reassuring, as it demonstrates that the effects of accretion are discernible in the gross statistical behavior of our study sample, even though multiple processes may be contributing at once to the observed variability, and even though the EW[Ca II] measurements that we use to identify the accretors were obtained years earlier (Hillenbrand et al. 1998).

3.2. Joint occurrences of optical and X-ray variability

Having found that accretion manifests itself in the level of optical variability of our sample, but not in the level of their X-ray variability, we next compare the *incidences* of optical and X-ray variability in these stars. We find statistically significant optical variability among 358/814 (44%) of the stars (Table 2) and statistically significant X-ray variability among 556/814 (68%) of the stars (§2.1.1). A Pearson χ^2 contingency-table test shows that the probability that optical and X-ray variability occur with the same frequency is less than 10^{-6} . In other words, a statistically significant fraction of stars that exhibit X-ray variability do not also exhibit optical variability in our data.

Conversely, we consider whether optically variable stars always exhibit X-ray variability. Of the 358 stars in our sample that we have identified as optically variable, 278 (78%) of them also exhibit X-ray variability (see Table 2). The likelihood that this fraction is consistent with 100% is again less than 10^{-6} . We can therefore state that, to the sensitivity available, the cause of optical variability cannot *at the same time* be the cause of X-ray variability for a significant fraction of the 814 observed stars. The two forms of variability simply do not always occur together during the 7 days of overlap between the optical and *Chandra* observations.

Perhaps the occurrences of optical and X-ray variability are more strongly related among those stars that are accreting, as one might expect if active accretion drives both forms of variability. To test this, we again segregate the stars in our sample into accretors and non-accretors, as defined earlier. Among the

²R is a freely available language and environment for statistical computing and graphics. See <http://www.r-project.org>.

accretors, we find simultaneous occurrences of optical and X-ray variability for 60 stars (40%), whereas for the non-accretors we find simultaneous occurrences of optical and X-ray variability for 64 stars (44%) (see Table 2). This small difference is not statistically significant (52% probability that they are not different) according to a Pearson χ^2 contingency-table test.

While we find clear evidence that optical and X-ray variability are not always linked to one another, and that the presence of active accretion does not increase the likelihood for an association between the two, this does not necessarily imply that the occurrences of optical and X-ray variability are completely independent of one another. In fact, we find that stars showing one form of variability are more likely to also show variability in the other. For example, whereas optical variability is found in 44% (358/814) of the overall study sample, this fraction increases to 50% among the stars in our sample that are X-ray variable (278/556), and 69% (178/258) of the X-ray non-variable stars are also optically non-variable (see Table 2). A Pearson χ^2 contingency-table test shows that the likelihood of the two measures of variability being independent of one another is less than 10^{-6} . Thus, optical and X-ray variability are, in fact, related. However, this relationship is not directly causal, as we now show.

3.3. Strength of optical and X-ray variability and their relation to X-ray luminosity

To explore the possible link between optical and X-ray variability further, we next examine how the *strength* of one may be related to the other. In Fig. 2, we plot the strength of optical variability, as measured by the J statistic (§2.1.2), versus the strength of X-ray variability, as measured by the BB analysis (§2.1.1). A Kendall’s τ test shows that the two measures are correlated at a high level of statistical significance, with the probability that they are not correlated being 3×10^{-6} . The same test conducted separately among the smaller sub-samples of accretors and non-accretors shows a correlation in the same sense, albeit at marginal levels of significance (Kendall’s τ probabilities of 0.08 and 0.009 for the accretors and non-accretors, respectively). Thus, we find that not only does the *presence* of one form of variability correlate with the other (see above), but that optical and X-ray variability are furthermore correlated in *strength*.

But do these statistical correlations between optical variability and X-ray variability imply a causal relationship between the two? The data suggest that this is *not* the case, and that the statistical relationship between optical and X-ray variability is in fact due to a mutual correlation—the first physical, the second observational—with X-ray *luminosity*.

X-ray luminosity (L_X) was found by Stassun et al. (2004) to be strongly correlated with optical variability in their analysis of all previous *Chandra* observations of PMS stars in the ONC. Specifically, they found that the ONC stars with the highest L_X also exhibited the highest levels of optical variability. This correlation is confirmed here, with a sample that is five times larger than that studied by Stassun et al. (2004). The correlation between J and L_X in our study sample (Fig. 3a) is highly statistically significant: The probability that J and L_X are uncorrelated, according to a Kendall’s τ test, is less than 10^{-6} . Importantly, we furthermore find that this correlation persists, at a less strong but still highly significant level, when we separately consider accretors and non-accretors.

At the same time, our sample exhibits a similar correlation between L_X and X-ray variability (Fig. 3b), with similarly high statistical significance as that between L_X and optical variability. In this case, however, the correlation appears to stem from an observational bias against detection of X-ray variability in stars with low L_X . Indeed, as shown in Fig. 3b, all of the stars for which the BB analysis finds no X-ray variability ($\text{BB}_{\text{max}}/\text{BB}_{\text{min}} = 1$) have $L_X < 10^{30} \text{ erg s}^{-1}$.

That optical and X-ray variability are both so strongly correlated with L_X suggests that this mutual correlation may be responsible for the correlation of optical and X-ray variability with another. To better understand these mutually correlated variables, we perform a multiple linear least-squares regression analysis on the strength of optical variability (J) simultaneously against the strength of X-ray variability (BB_{\max}/BB_{\min}) and L_X . The regression coefficient for L_X is found to be statistically significant (null hypothesis probability of 5×10^{-6}), but the coefficient for BB_{\max}/BB_{\min} is not (null hypothesis probability of 0.34). Similarly regressing BB_{\max}/BB_{\min} simultaneously against J and L_X , we find that the L_X coefficient is statistically significant (null hypothesis probability of less than 10^{-6}) but that the J coefficient is not (null hypothesis probability of 0.34). The regressions of J and BB_{\max}/BB_{\min} vs. L_X are represented by dashed lines in Fig. 3.

Thus, the relationship between optical and X-ray variability in our sample is, in fact, fully explained by the mutual correlations of J and BB_{\max}/BB_{\min} with L_X . Controlling for this mutual correlation with L_X , we find no statistically significant residual correlation of optical and X-ray variability with one another. Optical and X-ray variability are evidently not causally related.

Even though the correlation of optical variability with L_X has a plausible physical explanation (stars that are more heavily spotted are also stronger X-ray emitters; Stassun et al. 2004), our finding that the correlation of X-ray variability with L_X is due to observational bias (Fig. 3b) raises the suspicion that the correlation of optical variability with L_X may be similarly spurious. For example, L_X is known to be very strongly correlated with bolometric luminosity (L_{bol}) in the COUP sample (Preibisch et al. 2005). If optical variability is in turn correlated with L_{bol} in a manner similar to the correlation of X-ray variability with L_X , then this may explain the correlation of optical variability with L_X as being non-physical.

To examine this possibility quantitatively, we again perform a multiple regression analysis, as above, but this time on J against L_{bol} and L_X . First of all, we find that optical variability is indeed correlated with L_{bol} , albeit weakly (null-hypothesis probability of 0.02), when we regress J against L_{bol} alone. However, something unexpected occurs when we include L_X as a regressor. The regression coefficient for L_{bol} becomes statistically insignificant (null-hypothesis probability of 0.76), whereas the coefficient for L_X is significant, and with a higher degree of significance (null-hypothesis probability of 0.004^3) than was the correlation of J with L_{bol} alone. In other words, controlling for the correlation of J with L_{bol} does *not* eliminate the correlation of J with L_X ; on the contrary, controlling for the correlation of J with L_X eliminates the correlation of J with L_{bol} . L_X is evidently the more fundamental correlate.

This somewhat surprising result reinforces the conclusion that optical variability is intrinsically related to X-ray luminosity in our study sample. Having considered in detail the mutual correlations of J with BB_{\max}/BB_{\min} , L_{bol} , and L_X , only the correlation between J and L_X remains. The correlation between optical variability and L_X is more significant even than the intuitive correlation of optical variability with accretion (§3.1). Indeed, after controlling for the influence of all other secondary variables, we find that *the strongest correlate of optical variability in our study sample is X-ray luminosity.*

³Note that the statistical significance of the correlation between J and L_X is lower here than in the multiple regression analysis of J on L_X and BB_{\max}/BB_{\min} . This is because the sample under consideration here is smaller (545 stars vs. 814 stars), since L_{bol} measurements are not available for all stars in the COUP database.

3.4. Summary

We find that optical and X-ray variability in our study sample are not causally related. This conclusion follows from an examination of the joint occurrences of time-averaged optical and X-ray variability, as well as their mutual correlations with one another and with other variables. We find definitive evidence that, on timescales of 7 d or less, optical variability does not always occur in the presence of X-ray variability, nor vice-versa. Even when the two forms of variability are present, non-accreting stars are just as likely to show both forms of variability as are stars that exhibit active accretion; that is, among stars exhibiting both optical and X-ray variability, accretion is evidently not the cause. At a more detailed level, we have performed a multiple regression analysis, controlling for the mutual correlations of optical and X-ray variability, both with one another and with bolometric and X-ray luminosity. This analysis reveals that, while statistically significant correlations exist among all of these measures, the fundamental correlation in this study is that between optical variability and X-ray luminosity. This correlation is furthermore independent of accretion, indicating again that accretion is not the cause.

4. Discussion

While magnetic activity, and therefore X-ray production, in late-type main-sequence stars is relatively well understood in terms of a rotation-driven dynamo (e.g. Schrijver & Zwaan 2000), whether stellar rotation is also at the heart of PMS X-ray production is a contested issue. In contrast to the strong “rotation-activity relationship” that is clearly present on the main sequence (Pallavicini et al. 1981; Jeffries 1999; Randich 2000; Pizzolato et al. 2003), a series of studies based on *Chandra* observations of a large sample of PMS stars in the Orion Nebula Cluster (ONC) failed to find any direct correlation between the stars’ rotation rates and their X-ray luminosities (Flaccomio, Micela, & Sciortino 2003b; Feigelson et al. 2003; Preibisch et al. 2005).

However, Stassun et al. (2004), in an analysis of all archival *Chandra* observations of PMS stars in the ONC, found indirect evidence hinting that a main-sequence-type rotation-activity relationship may in fact be driving PMS X-ray production after all. They found a statistically significant, positive correlation between stellar rotation period and L_X , suggesting that these stars are on the “super-saturated” portion of the rotation-activity relation, consistent with their Rossby numbers. They furthermore found that the sample of ONC stars with known rotation periods is significantly biased to high L_X ; stars whose rotation periods are unknown, and which have lower L_X , may thus represent the unseen “linear” portion of the rotation-activity relation. Preibisch et al. (2005) and Rebull et al. (2006) have since confirmed these findings in different Orion samples.

The results of the present study lend further support for an interpretation in which accretion is *not* a significant source of X-ray production in PMS stars. Accretion, as traced by emission in Ca II, does not manifest itself in the X-ray variability of our study sample (§3.1). And while accretion *is* manifested in the *optical* variability of these stars as expected, a multiple regression analysis finds that X-ray variability is not correlated with this optical variability (§3.3). Moreover, we have found very few cases in our study sample in which the optical and X-ray variability are correlated in time (Paper I).

That we find so little evidence for accretion as a dominant source of X-rays in young stars suggests that we look to other possible X-ray production mechanisms. Indeed, there are now strong indications that X-ray production is intimately related in some way to the presence of magnetically active surface regions on these stars. The evidence for the existence of magnetically active surface regions on PMS stars is abundant. Several important studies of Zeeman broadening in the photospheric spectral lines of PMS stars

(e.g. Johns-Krull et al. 1999; Guenther et al. 1999; Johns-Krull, Valenti, & Saar 2004), as well as Doppler imaging of their surfaces (e.g. Rice & Strassmeier 1996; Johns-Krull & Hatzes 1997), provide direct proof of the existence of strong surface fields. Moreover, the X-ray flares observed in the COUP study can only be reasonably explained as reconnection events in strong stellar fields (Feigelson et al. 2006). In addition, numerous photometric studies of PMS stars have relied upon the presence of surface features to measure these stars’ rotation periods (e.g. Stassun et al. 1999; Rebull 2001; Herbst et al. 2002). The stability of these features over timescales of up to several years strongly suggests that these features are in many cases “starspots” presumably analogous to dark spots on the Sun.

Stassun et al. (2004) found that PMS stars in the ONC exhibit a highly statistically significant correlation between the strength of their optical variability (taken to be a measure of the stars’ “spottedness”) and their X-ray luminosities, in the sense that the least X-ray luminous stars are those with the smallest amount of spottedness. This finding led those authors to infer a causal connection between X-ray emission and the presence of starspots, leading to the conclusion that solar-analog surface magnetic activity driving hot coronae is the primary source of X-ray production in PMS stars. However, the possibility remained that the correlation between optical variability and X-ray luminosity was driven by accretion.

The results of the present study firmly corroborate the correlation between optical variability and X-ray luminosity (i.e. Fig. 3)—indeed, optical variability is the strongest correlate of X-ray luminosity in the COUP study sample (§3.3)—and furthermore show that this correlation exists regardless of whether the stars under consideration are accreting or non-accreting (§3.1). This finding contradicts models in which the observed X-ray emission is produced primarily by accretion, and instead bolsters support for the role of non-accretion-related, optically active magnetic regions (i.e. spots) in the production of PMS X-rays.

A small number of the stars in our sample evince periodic X-ray variability with a periodicity that is very similar to the observed periods in the optical (Flaccomio et al. 2005). In these cases the sites of X-ray emission may be predominantly co-spatial with magnetic surface spots. However, the association of X-ray production with magnetic spots does not manifest itself in a time-correlated way for most stars in our sample (Paper I), indicating that the X-ray emitting coronae in PMS stars generally have spatial structures that little reflect the spatial distribution of magnetic footpoints in the underlying photosphere.

These conclusions are consistent with recent studies of TTS magnetic field structures. For example, Jardine et al. (2006) find that a variety of field topologies are required to explain the observed scatter of emission measures of COUP stars, ranging from simple dipole fields to much more complex configurations. As discussed by those authors, the more complex field configurations are characterized by coronal gas that is confined to compact loops covering a large fraction of the stellar surface. Coronal emission arising from such a topology will have a relatively low X-ray luminosity by virtue of its compact size, and the footpoints of the multi-polar field will produce correspondingly small spots that are more-or-less uniformly distributed on the stellar surface (cf. Fig. 8 in Jardine et al. 2006), resulting in a relatively low-amplitude spot signal in the optical. The reverse will be true for a star whose coronal emission arises in a more extended, more dipolar field, rooted in a small number of footpoints (spots) that are more asymmetrically distributed on the stellar surface; such a configuration will produce a high X-ray luminosity together with strong optical variability. Thus, given a large ensemble of PMS stars with a range of field configurations, a strong correlation between X-ray luminosity and optical “spottedness,” as we have found here, may naturally follow.

5. Conclusions

We have presented a combined analysis of time-averaged optical and X-ray variability for more than 800 pre-main-sequence (PMS) stars in the Orion Nebula Cluster (ONC) with the aim of elucidating the origins of X-ray production in PMS stars. This study complements and extends the analysis of time-correlated variability in this same sample reported in Stassun et al. (2006).

Combining the results of these two studies, we find very little evidence to suggest a direct physical link between the sources of optical and X-ray variability in these stars. Whether we consider time-correlated behavior between the individual stars’ simultaneous optical and X-ray light curves, whether we consider the optical and X-ray variability properties of our study sample as a statistical ensemble, whether we segregate the stars according to their accretion properties, we arrive at the same conclusion: the sites of optical and X-ray variability in PMS stars are not—for the vast majority of stars—instantaneously one and the same. An interpretation in which accretion is a dominant source of X-ray production in PMS stars is not supported by the data.

Instead, the data provide strong support for an interpretation in which X-ray production in PMS stars is intimately connected with the presence and strength of optically variable, magnetic regions on their surfaces (i.e., spots). Indeed, after controlling for the influence of all other secondary variables, including accretion, we find that the strongest correlate of X-ray luminosity in our sample is spottedness (as measured by optical variability, after controlling for accretion). Our interpretation is that solar-analog magnetic activity is the primary, common driving mechanism of both optical variability and X-ray production in these stars. The fact that this relationship between spottedness and X-ray production does not, in the vast majority of cases, manifest itself in a time-correlated way (Paper I) suggests that the optical spots represent the footpoints of complex magnetic topologies that heat solar-analog coronae, as suggested by Jardine et al. (2006).

It is a pleasure to acknowledge the *Chandra* Orion Ultradeep Project (COUP) team, supported by *Chandra* Guest Observer grant SAO GO3–4009A (PI: E. Feigelson). This work is also supported by an NSF Career award (AST–0349075), and by a Cottrell Scholar award from the Research Corporation, to K. G. S.

Facility: CXO(ACIS)

REFERENCES

- Audard, M., Briggs, K., Grosso, N., Guedel, M., Scelsi, L., Bouvier, J., & Telleschi, A. 2007, *A&A*, in press
- Feigelson, E. D., Gaffney, J. A., Garmire, G., Hillenbrand, L. A., Townsley, L. 2003, *ApJ*, 584, 911
- Feigelson, E., Townsley, L., Gudel, M., & Stassun, K. 2006, *Protostars & Planets V*, in press
- Flaccomio, E., Micela, G., Sciortino, S., Feigelson, E. D., Herbst, W., Favata, F., Harnden, F. R., & Vrtillek, S. D. 2005, *ApJS*, 160, 450
- Flaccomio, E., Micela, G., & Sciortino, S. 2003b, *A&A*, 402, 277
- Flaccomio, E., Damiani, F., Micela, G., Sciortino, S., Harnden, F. R., Murray, S. S., & Wolk, S. J. 2003, *ApJ*, 582, 398
- Getman, K. V., et al. 2005, *ApJS*, 160, 319

- Glassgold, A. E., Feigelson, E. D., & Montmerle, T. 2000, *Protostars and Planets IV*, 429
- Guenther, E. W., Lehmann, H., Emerson, J. P., & Staude, J. 1999, *A&A*, 341, 768
- Herbst, W., Bailer-Jones, C. A. L., Mundt, R., Meisenheimer, K., & Wackermann, R. 2002, *A&A*, 396, 513
- Herbst, W., Herbst, D. K., Grossman, E. J., & Weinstein, D. 1994, *AJ*, 108, 1906
- Hillenbrand, L. A. 1997, *AJ*, 113, 1733
- Hillenbrand, L. A., Strom, S. E., Calvet, N., Merrill, K. M., Gatley, I., Makidon, R. B., Meyer, M. R., & Skrutskie, M. F. 1998, *AJ*, 116, 1816
- Jardine, M., Cameron, A. C., Donati, J.-F., Gregory, S. G., & Wood, K. 2006, *MNRAS*, 367, 917
- Jeffries, R.D. 1999, *ASP Conf. Ser. 158: Solar and Stellar Activity: Similarities and Differences*, 75
- Johns-Krull, C. M., Valenti, J. A., & Saar, S. H. 2004, *ApJ*, 617, 1204
- Johns-Krull, C. M., Valenti, J. A., & Koresko, C. 1999, *ApJ*, 516, 900
- Johns-Krull, C. M., & Hatzes, A. P. 1997, *ApJ*, 487, 896
- Kastner, J. H., Huenemoerder, D. P., Schulz, N. S., Canizares, C. R., & Weintraub, D. A. 2002, *ApJ*, 567, 434
- Pallavicini, R., Golub, L., Rosner, R., Vaiana, G. S., Ayres, T., & Linsky, J. L. 1981, *ApJ*, 248, 279
- Pizzolato, N., Maggio, A., Micela, G., Sciortino, S., & Ventura, P. 2003, *A&A*, 397, 147
- Preibisch, T., et al. 2005, *ApJS*, 160, 401
- Randich, S. 2000, *ASP Conf. Ser. 198: Stellar Clusters and Associations: Convection, Rotation, and Dynamics*, 401
- Rebull, L. M., Stauffer, J. R., Ramirez, S. V., Flaccomio, E., Sciortino, S., Micela, G., Strom, S. E., & Wolff, S. C. 2006, *AJ*, 131, 2934
- Rebull, L. M. 2001, *AJ*, 121, 1676
- Rice, J. B., & Strassmeier, K. G. 1996, *A&A*, 316, 164
- Scargle, J. D. 1998, *ApJ*, 504, 405
- Schrijver, C. J., & Zwaan, C. 2000, *Solar and stellar magnetic activity*. New York: Cambridge University Press, 2000. (Cambridge astrophysics series; 34)
- Sicilia-Aguilar, A., et al. 2005, *AJ*, 129, 363
- Stassun, K. G., Mathieu, R. D., Mazeh, T., & Vrba, F. J. 1999, *AJ*, 117, 2941
- Stassun, K. G., Ardila, D. R., Barsony, M., Basri, G., & Mathieu, R. D. 2004, *AJ*, 127, 3537
- Stassun, K. G., van den Berg, M., Feigelson, E. D., & Flaccomio, E. 2006, *ApJ*, in press (Paper I)
- Stelzer, B., & Schmitt, J. H. M. M. 2004, *A&A*, 418, 687

Stetson, P. B. 1996, PASP, 108, 851

Table 1. Optical and X-ray Variability in Study Sample

COUP	Opt. ^a	J^b	$\log P_{\text{KS}}^c$	BB ^d	Ca II ^e
6	40	1.65	≤ -4.00	11.5	0.0
7	45	0.51	≤ -4.00	11.3	...
9	46	1.21	≤ -4.00	81.8	...
10	48	0.59	-3.00	65.0	1.0
11	50	35.44	≤ -4.00	29.5	-14.6
12	51	10.80	≤ -4.00	7.2	0.0
13	53	4.06	-1.01	1.0	1.5
14	54	0.85	-2.70	3.2	0.0
15	55	8.85	≤ -4.00	4.6	1.0
16	3062	1.03	-0.26	1.0	-3.2
17	63	10.62	≤ -4.00	16.9	1.9
20	70	0.29	-2.85	4.1	0.0
21	71	0.45	≤ -4.00	3.3	0.0
23	75	0.77	≤ -4.00	15.8	...
26	10251	1.61	-1.17	1.0	...
27	77	11.57	≤ -4.00	11.6	1.8
28	81	9.18	≤ -4.00	68.6	1.6
29	83	9.92	≤ -4.00	4.2	-9.2
30	84	1.15	-0.47	1.0	0.0
33	10259	-0.52	-0.96	1.0	...
37	90	-0.13	-1.70	1.0	0.7
40	92	0.60	≤ -4.00	52.9	0.0
41	98	-0.53	≤ -4.00	67.1	0.0
43	99	25.76	≤ -4.00	51.0	1.4
44	104	8.99	≤ -4.00	4.3	-10.7
45	102	9.27	-0.56	1.0	0.0
46	105	-0.46	-1.60	1.0	0.0
47	106	1.10	≤ -4.00	3.4	1.5
49	107	6.22	≤ -4.00	3.3	-9.6
50	110	0.02	-1.00	1.0	0.0
54	113	22.49	≤ -4.00	4.9	-1.0
55	114	15.89	≤ -4.00	6.4	-1.4
57	116	1.44	≤ -4.00	4.0	1.6
58	117	6.34	-2.60	9.2	-6.3
59	10281	1.15	≤ -4.00	2.1	...
60	120	1.30	-2.49	1.6	1.0
62	123	16.29	≤ -4.00	26.8	0.0
64	124	-0.56	≤ -4.00	8.2	0.8
65	125	7.36	≤ -4.00	17.0	0.4
66	127	10.92	≤ -4.00	30.4	-2.8
67	128	1.24	≤ -4.00	13.0	0.0
68	130	-0.47	-2.08	3.5	...
69	132	1.63	≤ -4.00	2.1	...
71	133	2.40	≤ -4.00	10.7	1.6
72	135	6.12	≤ -4.00	1.9	-2.3
73	134	1.47	-1.83	3.4	...
74	137	1.85	≤ -4.00	3.2	...
75	136	21.94	-3.52	1.8	...
77	138	6.31	-1.01	1.0	-2.8
80	10294	0.35	-0.61	1.0	...
85	143	0.20	-1.95	1.0	-2.3
86	144	-0.39	-1.42	1.0	0.0
88	145	-0.15	≤ -4.00	183.3	...
89	146	1.77	≤ -4.00	28.7	0.0
90	148	1.45	≤ -4.00	415.2	1.6

Table 1—Continued

COUP	Opt. ^a	J^b	$\log P_{\text{KS}}^c$	BB ^d	Ca II ^e
94	149	1.50	−1.14	2.9	−23.7
95	151	−0.11	−0.29	1.0	−5.3
96	152	1.80	≤ -4.00	33.9	2.6
97	3111	1.96	≤ -4.00	13.8	−3.4
100	153	0.70	≤ -4.00	11.1	...
101	155	2.20	≤ -4.00	650.4	2.9
102	3046	0.76	−1.61	1.0	0.0
107	157	0.98	≤ -4.00	5.8	...
108	158	1.02	≤ -4.00	16.7	1.5
109	159	1.77	≤ -4.00	3.9	0.3
110	10308	0.45	≤ -4.00	20.5	...
112	164	5.65	≤ -4.00	69.5	−0.7
113	165	15.86	≤ -4.00	11.6	...
114	168	0.66	−2.42	4.1	0.0
115	167	0.09	≤ -4.00	8.2	1.4
117	169	6.62	≤ -4.00	32.2	...
118	171	0.44	≤ -4.00	4.3	0.4
119	174	1.63	−1.85	1.0	3.7
122	175	19.54	≤ -4.00	204.8	0.0
123	176	4.45	≤ -4.00	33.7	0.8
124	176	4.45	≤ -4.00	18.1	0.8
125	181	0.23	≤ -4.00	2.8	0.8
126	177	0.77	≤ -4.00	38.8	0.9
127	182	−0.12	−0.17	1.0	...
128	183	1.46	−0.48	1.0	0.0
130	184	0.56	≤ -4.00	3.2	1.6
131	187	2.45	≤ -4.00	44.8	1.4
132	188	1.70	≤ -4.00	33.6	0.0
133	189	0.49	−0.18	1.0	0.0
134	190	−0.09	−3.70	7.8	2.0
137	191	3.14	≤ -4.00	6.6	0.0
139	192	17.46	≤ -4.00	12.7	0.9
141	193	6.90	≤ -4.00	30.4	−17.8
142	197	0.79	≤ -4.00	64.4	...
143	196	2.84	≤ -4.00	11.4	1.2
144	5106	5.95	≤ -4.00	7.5	0.0
147	198	5.43	≤ -4.00	15.0	−1.0
148	200	1.08	−0.26	1.0	0.0
149	202	2.59	−1.34	1.0	−2.1
150	201	0.61	≤ -4.00	21.9	1.5
152	206	3.47	≤ -4.00	14.5	...
153	209	1.65	−0.71	1.0	...
154	205	0.60	≤ -4.00	6.0	0.0
157	207	1.15	−0.45	1.0	...
158	208	3.03	≤ -4.00	4.2	0.0
159	210	4.88	≤ -4.00	156.2	−0.5
161	211	4.68	≤ -4.00	5.4	1.4
164	213	−0.34	−0.73	1.0	0.6
166	212	0.23	≤ -4.00	2.2	0.0
168	215	0.15	−3.40	6.1	...
169	218	1.74	≤ -4.00	2.1	0.0
171	217	−0.02	−0.11	1.0	0.0
173	220	4.77	≤ -4.00	17.5	1.0
174	222	4.04	≤ -4.00	13.2	1.2
176	3138	0.97	−0.94	1.9	...

Table 1—Continued

COUP	Opt. ^a	J^b	$\log P_{\text{KS}}^c$	BB ^d	Ca II ^e
177	223a	2.75	−2.96	19.0	2.0
180	224	4.58	−1.05	1.0	−4.9
181	227	0.75	−0.49	1.0	...
183	226	0.96	≤ -4.00	17.6	0.0
187	230	1.05	−0.71	1.0	0.0
188	232	18.72	≤ -4.00	15.5	...
189	229	6.92	≤ -4.00	1.3	2.1
190	231	4.87	−0.52	1.0	0.0
192	5042	0.54	≤ -4.00	14.9	...
193	233	1.67	−0.63	1.0	−4.9
194	234	−0.39	−0.03	1.0	0.0
197	235	26.74	≤ -4.00	4.3	...
199	5100	2.96	≤ -4.00	49.2	−18.3
200	236	3.49	−0.71	1.0	...
201	237	6.23	≤ -4.00	3.9	0.0
202	239	8.59	≤ -4.00	12.1	1.5
205	243	0.82	≤ -4.00	22.0	1.2
206	10362	0.75	−0.17	1.0	...
207	241	1.10	−0.05	1.0	...
208	244	0.19	−3.52	2.5	−1.7
212	245	5.27	−1.23	1.0	−5.8
214	248	20.68	≤ -4.00	15.6	−0.9
217	249	27.50	≤ -4.00	23.6	1.7
218	250	2.36	≤ -4.00	9.6	0.9
219	254	3.15	−1.71	1.0	5.6
221	251	0.72	−3.70	2.3	2.0
222	256	0.50	≤ -4.00	9.0	2.1
223	253	15.62	≤ -4.00	20.9	1.7
226	258	8.79	≤ -4.00	88.0	1.2
227	259	4.93	−1.87	1.5	−2.7
228	257	0.12	−1.53	1.0	0.0
230	10368	0.58	≤ -4.00	6.6	...
232	261	8.39	−2.05	1.0	...
234	5112	0.97	−1.05	1.0	...
235	262	−0.12	−0.19	1.0	0.0
236	265	3.80	≤ -4.00	3.9	0.0
237	5096	1.31	≤ -4.00	1.9	0.0
238	266	10.99	≤ -4.00	14.3	...
240	270	−0.19	−1.34	2.7	0.0
241	268	5.58	≤ -4.00	13.5	2.8
242	10370	1.52	≤ -4.00	38.3	...
243	272	3.49	−1.83	7.8	−2.2
244	3040	−0.44	≤ -4.00	9.5	...
245	273	3.65	≤ -4.00	30.4	−15.9
246	277	2.07	−2.27	1.0	0.0
248	279	1.65	−0.08	1.0	−3.0
249	276	1.15	≤ -4.00	56.2	1.1
250	278	30.56	≤ -4.00	28.9	−9.6
252	275a	3.77	≤ -4.00	15.1	1.8
253	280	0.55	≤ -4.00	228.3	1.4
255	281	0.77	≤ -4.00	4.9	1.3
256	283	0.26	≤ -4.00	2.7	0.0
259	285	1.29	≤ -4.00	6.2	−0.4
260	3064	1.14	≤ -4.00	14.1	...
262	286	0.69	≤ -4.00	10.1	2.3

Table 1—Continued

COUP	Opt. ^a	J^b	$\log P_{\text{KS}}^c$	BB ^d	Ca II ^e
264	288	1.03	−1.14	1.0	0.9
265	287	0.09	−1.92	1.0	−4.3
266	290	0.82	≤ −4.00	2.6	...
270	291	1.38	≤ −4.00	17.6	1.5
271	292	0.80	−2.41	3.3	0.0
273	5159	1.77	−0.19	1.0	...
275	296	0.38	−1.08	1.0	−3.2
276	298	0.66	≤ −4.00	58.5	...
279	299	0.92	−0.16	1.0	...
281	5064	0.44	−0.18	1.0	0.0
283	300	1.20	≤ −4.00	185.8	0.0
286	302	0.73	−2.54	6.5	...
287	5138	0.70	−0.25	1.0	...
289	303	0.55	−0.54	1.0	...
290	304	0.87	≤ −4.00	376.8	0.6
291	5075	5.74	−1.36	1.0	...
294	306	1.40	−0.46	2.1	0.0
296	307	0.82	−2.13	1.0	1.7
298	311	3.63	≤ −4.00	3.0	0.0
300	309	3.05	−1.37	1.0	0.8
301	313	22.07	≤ −4.00	259.3	0.5
304	314	1.69	≤ −4.00	38.1	...
305	318	0.59	−1.32	1.0	0.8
309	317	2.36	≤ −4.00	11.3	...
310	319	0.64	≤ −4.00	13.5	8.9
314	320	7.36	≤ −4.00	23.4	0.3
316	322	1.35	≤ −4.00	2.9	−1.8
318	323	14.06	−3.30	12.2	0.8
320	10395	0.46	−0.55	1.0	...
321	324	0.89	≤ −4.00	34.8	−3.3
322	3072	1.15	≤ −4.00	31.3	...
323	326	1.21	≤ −4.00	28.8	2.0
325	328	29.11	≤ −4.00	9.4	0.0
326	3045	3.67	−1.31	1.0	...
328	330	1.97	≤ −4.00	2.0	1.8
331	3134	0.16	≤ −4.00	181.2	...
333	331	0.75	≤ −4.00	50.0	...
336	332	1.11	−2.60	1.0	−0.9
339	335	0.88	≤ −4.00	7.9	−26.0
340	333	0.50	≤ −4.00	2.9	3.7
341	334	7.49	−0.76	1.0	−4.8
342	336	0.85	≤ −4.00	8.9	...
343	337	4.84	≤ −4.00	21.5	1.9
346	338	2.42	≤ −4.00	12.7	0.0
349	1772	1.03	−1.82	1.0	...
350	9002	0.96	−1.06	1.0	...
358	340	0.10	≤ −4.00	57.0	...
362	339	3.97	≤ −4.00	26.1	0.0
363	342	3.35	−0.55	1.0	...
365	341	0.62	≤ −4.00	21.3	0.0
367	3047	1.19	≤ −4.00	6.3	0.0
368	343	3.65	≤ −4.00	3.0	0.9
378	345	2.98	≤ −4.00	3.7	0.0
379	3104	1.00	≤ −4.00	2.8	...
380	5142	0.92	−1.18	1.0	...

Table 1—Continued

COUP	Opt. ^a	J^b	$\log P_{\text{KS}}^c$	BB ^d	Ca II ^e
382	347	0.49	≤ -4.00	23.0	0.0
383	...	1.73	-1.39	1.0	...
385	349	1.95	≤ -4.00	32.1	0.0
387	348	7.37	≤ -4.00	8.7	...
394	352	0.58	≤ -4.00	3.2	1.9
395	354	0.50	≤ -4.00	21.4	1.3
399	3102	-0.05	≤ -4.00	201.5	...
403	355	2.23	≤ -4.00	43.0	-6.2
404	356	1.57	≤ -4.00	13.4	-1.3
405	357	0.80	-3.10	4.0	0.0
408	10415	-0.18	-1.25	1.0	...
410	359	0.30	≤ -4.00	18.3	...
411	3098	0.59	-1.54	1.0	...
414	358	1.95	≤ -4.00	97.1	0.0
416	...	4.28	-2.10	1.0	...
417	361	4.10	≤ -4.00	25.2	...
421	3005	-0.42	-0.18	1.0	0.0
430	365	1.31	≤ -4.00	33.8	...
431	364	-0.14	≤ -4.00	12.0	...
433	3070	2.51	-0.17	1.0	...
434	366	0.27	-0.55	1.0	-2.7
437	371	0.26	-1.15	1.0	...
439	369	3.68	≤ -4.00	2.3	...
442	9008	0.86	≤ -4.00	8.1	0.0
443	368	2.65	-0.51	1.0	...
446	367	0.23	≤ -4.00	3.8	...
449	3058	0.43	≤ -4.00	26.5	0.0
450	...	2.71	≤ -4.00	42.5	...
452	370	0.94	≤ -4.00	6.9	1.4
454	373	6.28	≤ -4.00	14.2	2.1
459	375	1.89	≤ -4.00	38.3	...
462	5132	0.86	-0.02	1.0	...
467	379	2.06	≤ -4.00	10.5	...
468	380	-0.45	≤ -4.00	74.7	...
470	378a	3.55	≤ -4.00	6.5	1.5
474	381	41.97	-2.96	7.1	0.0
478	...	2.28	-3.10	2.0	...
480	...	4.28	-0.76	1.0	...
482	5074	-0.01	-3.52	3.1	...
485	387	0.92	≤ -4.00	93.2	-1.0
486	382	0.20	≤ -4.00	5.0	0.0
487	...	1.52	≤ -4.00	167.7	...
488	385	-0.76	≤ -4.00	3.7	...
489	383	3.70	-2.31	4.3	0.0
490	386	-0.35	≤ -4.00	69.9	1.2
492	389	2.54	≤ -4.00	3.5	4.0
493	390	1.12	≤ -4.00	2.0	...
497	...	1.47	-2.59	1.0	...
498	392	-0.17	-1.09	1.0	0.0
499	388	7.64	≤ -4.00	9.4	1.2
501	391	8.82	≤ -4.00	14.3	-25.2
513	397	-0.08	-0.16	1.0	...
514	393	-0.75	≤ -4.00	4.8	...
515	394	3.14	≤ -4.00	16.4	0.0
516	9028	0.29	≤ -4.00	24.8	-2.8

Table 1—Continued

COUP	Opt. ^a	J^b	$\log P_{\text{KS}}^c$	BB ^d	Ca II ^e
517	395	1.40	≤ -4.00	4.2	−6.2
518	9029	0.53	≤ -4.00	3.2	1.5
522	9032	2.09	≤ -4.00	13.9	−30.4
527	405	1.66	≤ -4.00	6.3	...
528	400	0.20	≤ -4.00	74.2	0.0
533	...	1.83	≤ -4.00	774.0	...
534	401	1.23	−0.82	1.0	−22.3
535	405	1.66	−2.06	3.5	...
536	403	1.20	≤ -4.00	11.3	1.6
538	404	0.91	−0.87	1.0	...
543	406	2.94	≤ -4.00	4.9	1.7
545	409	8.66	≤ -4.00	34.2	11.3
546	416	1.00	≤ -4.00	5.6	1.2
547	408	1.22	−0.98	1.0	2.5
550	9047	1.25	≤ -4.00	138.3	2.1
551	411	1.67	≤ -4.00	9.4	...
553	412	1.01	≤ -4.00	81.7	−3.5
557	415	0.05	≤ -4.00	27.8	1.8
558	418	1.59	≤ -4.00	5.3	...
560	...	0.11	≤ -4.00	3.4	...
561	413	3.63	≤ -4.00	12.0	1.0
562	9048	0.72	−1.61	1.0	−5.6
565	417	3.52	≤ -4.00	3.0	0.0
566	422	5.06	≤ -4.00	57.7	...
567	421	2.02	≤ -4.00	10.8	−3.5
569	419	1.40	−2.12	1.0	...
573	420	1.22	−1.01	1.0	...
579	423	2.39	≤ -4.00	79.9	−17.4
584	427	1.46	−1.19	1.0	...
585	428	0.42	≤ -4.00	2.5	1.4
586	425	0.28	≤ -4.00	99.8	...
593	...	0.95	≤ -4.00	4.2	...
597	429	6.02	≤ -4.00	20.1	4.5
600	432	0.98	≤ -4.00	45.4	...
602	431	0.38	≤ -4.00	10.9	...
604	3093	0.00	−1.88	1.7	...
605	3099	−0.02	−1.53	1.0	0.0
606	434	0.12	≤ -4.00	2.3	...
612	435a	1.84	≤ -4.00	1.5	...
616	437	2.72	≤ -4.00	3.0	1.4
618	438	1.45	−3.10	8.5	...
621	...	2.84	≤ -4.00	7.1	...
622	9063	0.86	≤ -4.00	30.0	...
625	...	2.01	≤ -4.00	8.8	...
626	439	2.53	≤ -4.00	19.3	0.7
631	441	2.14	≤ -4.00	4.2	0.7
632	...	1.34	−0.50	1.0	...
634	443	1.79	≤ -4.00	36.2	−1.5
636	447	2.05	−1.67	1.0	...
638	442	1.28	−0.22	1.0	−1.4
643	446	0.02	−0.40	1.0	0.0
645	445a	0.87	≤ -4.00	8.2	4.4
648	448	0.53	≤ -4.00	3.5	...
649	9069	−0.09	≤ -4.00	61.9	0.0
651	444	1.00	−0.30	1.0	...

Table 1—Continued

COUP	Opt. ^a	J^b	$\log P_{\text{KS}}^c$	BB ^d	Ca II ^e
653	450	1.87	≤ -4.00	6.4	0.8
658	451	0.32	≤ -4.00	6.5	−8.4
663	452	0.49	≤ -4.00	3.2	...
665	...	0.90	≤ -4.00	1.6	...
666	453	0.60	≤ -4.00	4.5	...
669	457	4.69	≤ -4.00	9.7	...
670	454	1.00	≤ -4.00	24.9	−1.0
672	456	0.96	≤ -4.00	8.1	...
682	463	12.94	≤ -4.00	80.8	...
684	464	2.64	−2.39	1.0	...
685	461	0.51	−3.70	14.2	...
686	9092	0.29	−0.58	1.0	−3.5
688	467	0.89	−2.37	4.4	0.7
689	468	1.53	≤ -4.00	8.0	1.0
694	462	0.28	−2.62	10.3	0.0
695	469	4.57	≤ -4.00	2.2	0.0
697	470	3.54	≤ -4.00	5.2	6.1
700	5177	2.82	≤ -4.00	3.8	...
701	471	9.36	≤ -4.00	3.9	...
703	...	0.60	−0.02	1.0	...
705	473	2.11	≤ -4.00	93.7	−31.3
707	476	0.97	≤ -4.00	9.7	1.6
708	475	0.52	≤ -4.00	32.8	...
710	3103	0.51	≤ -4.00	47.8	...
711	477	1.19	≤ -4.00	12.2	1.3
717	5178	0.81	−0.44	1.0	...
718	478	4.82	≤ -4.00	12.8	...
720	3032	−0.20	≤ -4.00	21.9	...
724	479	1.44	≤ -4.00	2.5	2.0
726	480	0.70	≤ -4.00	2.4	...
727	9108	0.51	−0.03	1.0	−9.3
728	482	1.63	≤ -4.00	36.2	−50.3
731	481	−0.42	−0.45	1.0	0.0
737	485	7.07	≤ -4.00	18.3	0.8
738	486	0.00	−0.03	1.0	0.0
739	490	0.52	≤ -4.00	31.5	−1.2
742	492	0.68	≤ -4.00	26.4	−0.9
743	494	0.28	−1.10	2.3	0.6
746	488a	1.34	−3.40	2.6	−6.5
748	9118	0.68	−0.35	1.0	−53.0
750	502	4.64	≤ -4.00	4.7	0.0
752	501	1.24	≤ -4.00	132.6	1.1
753	487	10.69	≤ -4.00	33.8	1.8
754	493	0.31	≤ -4.00	6.8	...
756	496	4.47	−3.22	1.9	−10.8
758	499	3.00	≤ -4.00	11.2	−12.3
761	504b	0.13	≤ -4.00	18.3	...
762	497	1.26	≤ -4.00	67.6	...
763	500	0.61	−0.84	1.0	0.5
768	503	0.11	≤ -4.00	4.4	−6.1
770	505	1.03	≤ -4.00	11.2	−13.7
771	9124	1.21	≤ -4.00	3.4	0.0
773	3016	0.79	≤ -4.00	23.2	...
776	9132	−0.15	≤ -4.00	2.6	−7.8
778	1863a	9.70	−1.16	1.0	...

Table 1—Continued

COUP	Opt. ^a	J^b	$\log P_{\text{KS}}^c$	BB ^d	Ca II ^e
782	9135	−0.26	≤ -4.00	2.9	...
783	507	0.50	≤ -4.00	14.3	−4.0
789	509a	0.92	≤ -4.00	121.5	...
790	3117	1.33	≤ -4.00	18.9	...
791	517	0.62	−1.27	1.0	0.0
792	518	0.79	−0.06	1.0	0.0
794	508	27.47	≤ -4.00	11.1	2.3
795	5056	−0.07	≤ -4.00	11.4	...
796	510	1.15	−3.00	3.3	−0.4
800	513	0.28	−0.85	3.8	−1.7
801	515	2.85	≤ -4.00	14.0	−1.2
803	516	1.69	≤ -4.00	90.8	1.8
807	519a	0.16	≤ -4.00	23.7	1.0
813	521	0.82	≤ -4.00	28.4	0.0
814	9147	1.86	≤ -4.00	9.3	−5.1
816	522	1.14	≤ -4.00	42.5	...
817	520	7.62	≤ -4.00	30.2	−10.6
821	527	1.55	≤ -4.00	12.8	0.8
822	3031	0.61	−0.11	1.0	...
825	9151	1.25	≤ -4.00	45.4	−6.2
826	524	1.47	≤ -4.00	19.9	...
830	523	0.20	−3.40	1.8	1.7
832	529	−1.50	≤ -4.00	2.5	...
839	3055	0.72	−2.14	4.3	...
844	532	1.58	−0.96	1.0	...
845	533	1.37	≤ -4.00	2.3	1.8
847	534	4.31	−2.00	1.0	−69.5
848	535	0.95	≤ -4.00	117.3	0.0
849	...	0.91	−3.52	8.8	...
851	528	0.52	−1.34	3.8	...
853	9163	1.68	−0.38	1.0	−4.6
854	536	0.45	≤ -4.00	22.7	1.7
855	538	4.56	≤ -4.00	3.0	1.1
856	537	1.45	≤ -4.00	2.8	−9.3
857	543	2.27	≤ -4.00	20.1	...
862	539	0.15	≤ -4.00	2.9	...
863	540	1.04	−0.26	1.0	...
864	546	0.57	−1.09	3.4	...
865	542	5.55	≤ -4.00	16.7	−1.0
867	544	2.02	≤ -4.00	15.0	1.6
870	9171	2.75	≤ -4.00	3.8	−11.1
871	547	1.89	≤ -4.00	9.4	0.0
876	548	3.35	−2.60	6.4	−3.6
881	551a	2.22	≤ -4.00	80.3	2.0
882	555	0.50	−0.70	1.0	−1.4
883	5047	−0.03	−0.40	1.0	...
887	9176	0.45	−1.60	1.0	...
888	9179	1.69	≤ -4.00	6.7	−1.9
889	556	0.54	≤ -4.00	8.9	...
891	550	2.33	≤ -4.00	49.2	1.8
899	553a	1.67	≤ -4.00	11.4	−0.7
901	557	28.29	≤ -4.00	2.4	−0.8
904	...	1.81	≤ -4.00	11.0	...
907	565	10.88	≤ -4.00	5.9	0.0
914	559	1.41	−3.22	6.9	−5.1

Table 1—Continued

COUP	Opt. ^a	J^b	$\log P_{\text{KS}}^c$	BB ^d	Ca II ^e
917	561	5.11	≤ -4.00	171.1	...
921	9201	4.68	-3.40	11.4	-3.0
922	562	0.87	≤ -4.00	6.4	-2.2
924	9199	0.77	≤ -4.00	12.4	...
926	571	11.01	≤ -4.00	1.0	-3.3
927	560	3.26	≤ -4.00	29.0	...
928	563	0.33	≤ -4.00	25.9	...
929	564	-0.47	≤ -4.00	58.7	...
932	567	-0.01	≤ -4.00	12.1	-1.7
935	9204	2.06	-0.97	1.0	-14.1
936	569	1.54	≤ -4.00	5.2	...
937	570a	4.55	≤ -4.00	2.8	...
938	573	1.79	≤ -4.00	136.4	0.0
939	566	0.53	≤ -4.00	11.0	...
942	9209	0.39	≤ -4.00	13.0	0.0
943	575	1.16	≤ -4.00	13.7	...
945	576	1.43	≤ -4.00	11.9	0.0
946	577	0.39	≤ -4.00	16.1	1.0
947	568	-0.10	-0.72	1.0	1.0
948	580	0.83	≤ -4.00	3.4	-7.7
949	572	-0.05	≤ -4.00	15.3	...
954	9220	0.77	-0.75	1.0	-1.8
955	582	1.80	-0.36	6.8	-4.2
956	581	2.87	≤ -4.00	1.8	...
957	9213	0.63	-0.90	1.0	...
958	583	-1.17	-1.01	1.0	3.1
960	590	0.21	≤ -4.00	441.0	0.0
962	584	0.70	-1.34	3.6	0.0
963	586	1.66	≤ -4.00	83.1	...
965	589	-0.13	≤ -4.00	1.4	-0.6
969	591	1.22	≤ -4.00	6.9	...
970	3140	0.20	≤ -4.00	50.1	...
971	585	1.13	≤ -4.00	21.9	1.8
972	9228	0.21	≤ -4.00	31.3	-2.0
974	592	5.06	-1.29	2.1	0.0
976	594	1.54	≤ -4.00	193.4	0.0
982	593	1.15	≤ -4.00	6.3	1.8
983	10541	1.86	-2.26	1.0	...
985	595	1.49	≤ -4.00	11.6	...
986	596	14.88	≤ -4.00	11.9	-7.7
987	9232	1.35	-0.13	1.0	-17.1
989	10543	0.98	-0.16	1.0	...
990	5058	2.97	≤ -4.00	2.3	...
992	600	0.24	≤ -4.00	3.7	...
993	598a	-0.68	≤ -4.00	7.2	-0.3
994	597	14.28	≤ -4.00	37.7	...
995	599	7.07	-1.29	1.0	2.8
997	603	4.78	≤ -4.00	39.5	...
1000	604	1.94	≤ -4.00	15.6	-19.0
1001	9238	1.36	-3.52	2.8	-17.9
1002	601	-0.21	≤ -4.00	28.4	2.5
1006	605	5.29	≤ -4.00	13.1	-2.3
1007	606	2.49	≤ -4.00	19.8	...
1008	9243	3.60	≤ -4.00	1.3	-4.2
1011	607	0.59	≤ -4.00	1.8	2.3

Table 1—Continued

COUP	Opt. ^a	J^b	$\log P_{\text{KS}}^c$	BB ^d	Ca II ^e
1012	9245	1.16	≤ -4.00	9.7	−15.3
1019	610	1.22	≤ -4.00	14.1	−5.8
1023	9250	6.02	≤ -4.00	3.8	0.6
1024	615	0.04	−0.13	1.0	−4.5
1025	5147	1.49	≤ -4.00	2.2	...
1026	612	6.39	−0.45	1.0	−24.7
1027	10553	−0.04	≤ -4.00	20.5	...
1028	613	0.92	≤ -4.00	12.2	...
1032	617	0.79	−0.36	1.0	21.4
1034	5041	1.36	−1.66	6.1	...
1036	616	0.84	−0.98	1.0	−3.3
1038	621	2.26	−0.28	1.0	...
1044	620	3.28	≤ -4.00	8.6	−2.8
1045	622	0.83	≤ -4.00	23.9	−7.0
1047	619	0.11	−0.13	1.0	0.0
1056	624	2.26	−2.89	3.3	0.0
1058	625	0.05	≤ -4.00	4.0	6.1
1059	632	3.28	−3.22	2.6	0.0
1060	628	1.12	≤ -4.00	2.2	...
1061	5066	0.68	≤ -4.00	62.4	...
1064	9256	3.99	−0.07	1.0	−10.4
1065	633	2.59	−2.72	1.0	...
1070	634	0.77	≤ -4.00	56.8	...
1071	631	4.23	≤ -4.00	6.2	1.6
1076	636	18.35	≤ -4.00	17.0	...
1077	638	2.61	−2.70	1.0	...
1080	629	3.06	≤ -4.00	25.0	−16.9
1083	637	2.19	≤ -4.00	11.7	...
1085	3075	0.95	≤ -4.00	10.3	...
1087	641	1.79	≤ -4.00	8.4	0.0
1088	642	0.79	−0.14	1.0	0.0
1089	635	0.10	≤ -4.00	1.6	0.0
1090	640	6.37	≤ -4.00	6.2	...
1093	649	1.16	−0.26	1.0	0.0
1095	5119	0.83	≤ -4.00	37.6	−5.0
1096	647	26.52	≤ -4.00	220.9	−5.0
1097	643	4.41	≤ -4.00	6.0	1.0
1100	645	1.56	≤ -4.00	3.9	13.6
1101	648a	−0.36	≤ -4.00	24.1	0.9
1102	653	0.05	−2.03	1.0	0.0
1103	651	0.77	≤ -4.00	16.7	...
1104	650	0.95	≤ -4.00	10.5	...
1107	652	1.09	−0.87	1.0	−8.2
1110	657	1.06	≤ -4.00	37.0	2.0
1111	659	2.79	≤ -4.00	33.4	...
1112	658	0.84	≤ -4.00	6.3	−7.6
1113	10582	1.22	−0.75	1.0	...
1114	655	1.47	≤ -4.00	20.4	−1.5
1116	660	−0.14	≤ -4.00	5.6	...
1117	661	0.97	≤ -4.00	9.0	2.1
1118	3106	2.02	−0.63	1.0	...
1120	662	3.89	−3.52	8.2	−1.0
1121	663	−0.24	−3.30	2.7	2.4
1122	665	1.23	≤ -4.00	500.7	−10.1
1124	9271	0.20	≤ -4.00	3.9	−4.4

Table 1—Continued

COUP	Opt. ^a	J^b	$\log P_{\text{KS}}^c$	BB ^d	Ca II ^e
1127	664	6.84	≤ -4.00	49.3	1.4
1130	669	1.94	≤ -4.00	2.0	1.8
1131	9272	1.46	≤ -4.00	16.3	...
1132	672	2.75	≤ -4.00	105.5	3.0
1134	673	0.92	≤ -4.00	26.6	1.3
1135	668	1.15	≤ -4.00	3.6	...
1138	9277	0.27	-1.57	1.0	0.0
1139	674	10.52	≤ -4.00	9.2	0.0
1140	9278	1.01	≤ -4.00	72.2	...
1141	9280	2.15	≤ -4.00	5.1	-4.6
1143	678	13.85	≤ -4.00	7.1	...
1144	680	-0.40	-0.46	1.0	...
1148	9283	1.48	-1.29	1.0	-6.8
1150	679	1.10	-0.54	1.0	-2.0
1151	683	3.35	≤ -4.00	6.6	1.9
1154	684	-0.43	≤ -4.00	12.7	0.0
1155	685	1.08	-0.36	1.0	-1.3
1158	687a	3.84	≤ -4.00	20.1	0.0
1161	690	2.30	≤ -4.00	9.3	1.5
1162	688	0.68	-3.22	8.7	...
1163	689	1.56	-0.99	1.0	0.0
1166	693	1.00	-2.29	6.5	-2.9
1167	694	1.93	≤ -4.00	3.8	-3.8
1169	695	-0.09	≤ -4.00	36.6	0.6
1171	697	1.32	≤ -4.00	16.0	...
1172	9293	-0.14	≤ -4.00	44.2	...
1174	698	2.91	-2.43	1.5	...
1177	692	-0.64	≤ -4.00	1.7	1.6
1178	691	0.35	≤ -4.00	13.5	0.0
1182	702	-0.22	-0.43	1.0	3.1
1184	5179	1.81	≤ -4.00	13.6	...
1185	3116	0.67	-0.47	1.0	...
1186	704	1.33	≤ -4.00	8.6	...
1187	3121	0.28	-0.33	1.0	...
1190	9298	1.21	-3.00	3.8	...
1191	9297	-0.07	≤ -4.00	160.9	-5.3
1193	707	10.08	≤ -4.00	12.3	...
1195	3034	0.16	-0.69	1.0	...
1199	706	-0.14	≤ -4.00	1.8	...
1201	9299	2.23	0.00	1.0	...
1202	709	0.33	≤ -4.00	7.9	2.8
1204	711	1.01	-2.06	1.0	0.0
1205	710	4.73	-0.68	1.0	-2.1
1206	716	3.14	≤ -4.00	8.1	-2.7
1207	715	1.21	≤ -4.00	28.9	0.0
1210	712	6.51	≤ -4.00	6.3	0.8
1212	713	1.78	≤ -4.00	12.8	...
1213	718	3.28	≤ -4.00	3.8	...
1214	720	-0.19	≤ -4.00	7.5	...
1216	721	5.34	≤ -4.00	13.4	-3.8
1217	5007	-0.31	-0.16	1.0	...
1218	714	0.48	-0.26	1.0	...
1219	717	2.61	≤ -4.00	9.1	0.0
1222	3023	2.11	-0.76	1.0	...
1231	723	7.81	≤ -4.00	18.4	-1.1

Table 1—Continued

COUP	Opt. ^a	J^b	$\log P_{\text{KS}}^c$	BB ^d	Ca II ^e
1233	727	4.96	≤ -4.00	10.4	0.8
1236	728	6.58	≤ -4.00	40.2	0.9
1239	5009	0.07	≤ -4.00	3.7	...
1241	3105	3.37	-0.13	1.0	...
1242	730	0.06	-1.03	1.0	...
1243	734	0.18	-0.27	1.0	...
1245	732	1.32	≤ -4.00	57.8	-15.8
1246	735	3.71	≤ -4.00	207.2	0.0
1247	5027	1.11	-0.18	1.0	...
1248	733	0.01	≤ -4.00	11.0	1.7
1252	736	2.50	≤ -4.00	81.2	1.6
1259	738	0.08	≤ -4.00	150.9	-0.3
1260	740	1.57	-0.93	1.0	-8.2
1261	741	-0.13	≤ -4.00	76.8	...
1262	737	1.98	-2.31	1.0	...
1263	743	12.62	-0.27	1.0	-2.0
1264	739	6.89	≤ -4.00	8.5	-1.8
1265	742	0.31	-2.54	1.0	...
1266	5131	0.88	0.00	1.0	...
1267	9312	0.72	≤ -4.00	61.3	...
1268	744	-0.14	≤ -4.00	82.7	-0.9
1269	747	-0.33	≤ -4.00	11.4	...
1271	746	0.24	≤ -4.00	29.7	0.6
1275	3087	2.35	≤ -4.00	4.6	-4.7
1276	...	1.78	≤ -4.00	136.2	...
1279	748a	1.43	≤ -4.00	21.6	-1.4
1280	9316	1.04	≤ -4.00	42.6	0.0
1281	750	3.08	≤ -4.00	2.8	0.0
1282	753	3.26	≤ -4.00	3.1	...
1286	3101	-0.34	-1.29	1.0	...
1287	10620	0.87	-0.27	1.0	...
1288	755	0.26	-1.15	1.0	0.0
1289	757	0.99	-1.42	1.0	...
1290	756	1.72	≤ -4.00	146.0	-2.0
1291	758	6.08	≤ -4.00	4.0	-2.0
1292	751	8.05	≤ -4.00	146.7	-3.0
1293	759	1.81	-0.63	1.0	...
1295	760a	11.28	-1.76	1.0	-8.5
1299	761	0.19	≤ -4.00	15.5	...
1302	762	12.33	≤ -4.00	19.4	-4.5
1305	763	2.82	≤ -4.00	85.1	0.8
1306	764	0.40	≤ -4.00	9.2	...
1307	10624	2.59	≤ -4.00	100.4	...
1309	766a	1.96	≤ -4.00	7.9	...
1311	769	1.53	≤ -4.00	4.1	...
1312	768	3.79	≤ -4.00	1.5	-14.8
1314	770	0.71	≤ -4.00	5.6	-3.7
1316	767	32.01	≤ -4.00	11.4	-1.8
1317	773	0.33	-0.87	1.0	...
1319	3128	0.28	-1.94	1.0	...
1323	775	-0.89	-2.89	3.4	0.0
1324	3095	4.71	≤ -4.00	111.7	...
1326	777	0.98	-3.70	10.2	2.5
1327	777	1.00	≤ -4.00	6.9	2.5
1328	776a	6.50	≤ -4.00	28.3	...

Table 1—Continued

COUP	Opt. ^a	J^b	$\log P_{\text{KS}}^c$	BB ^d	Ca II ^e
1329	3079	0.53	≤ -4.00	46.2	...
1332	5059	0.49	-0.10	1.0	...
1333	787	25.02	≤ -4.00	5.2	0.6
1334	788	14.80	-0.17	8.4	0.0
1335	782	5.40	≤ -4.00	22.6	-2.5
1336	786	5.55	≤ -4.00	13.9	0.0
1341	791	0.49	≤ -4.00	24.7	...
1342	792	3.97	≤ -4.00	6.1	1.4
1343	793	3.17	≤ -4.00	68.3	...
1344	3069	2.03	≤ -4.00	15.0	...
1345	3090	0.66	-1.17	1.0	0.0
1347	796	24.80	-0.59	1.0	-9.3
1350	795	3.28	≤ -4.00	12.7	1.7
1354	799	1.90	≤ -4.00	11.1	...
1355	798	4.99	≤ -4.00	4.7	0.0
1356	3021	1.28	≤ -4.00	4.7	...
1358	800	0.15	-0.67	1.0	0.0
1361	802	4.10	-0.18	1.0	...
1362	801	-0.29	≤ -4.00	3.7	...
1363	797	13.11	-1.72	6.5	...
1366	3027	10.37	-1.29	1.0	...
1370	10649	0.48	≤ -4.00	3.0	...
1371	10653	-0.63	-2.24	1.0	...
1372	807	-0.02	-3.70	9.4	2.1
1373	806	0.69	-1.28	1.0	2.5
1374	805	1.50	≤ -4.00	46.7	...
1378	812	0.38	-0.87	1.0	...
1380	810	2.16	≤ -4.00	19.3	...
1382	811a	17.77	≤ -4.00	9.1	0.0
1384	813	4.24	≤ -4.00	20.0	1.9
1385	10659	0.67	-0.98	1.0	...
1387	815	4.65	≤ -4.00	36.1	0.0
1388	817	-0.11	≤ -4.00	28.5	...
1391	816	3.18	≤ -4.00	9.7	1.4
1394	3077	0.59	-0.90	1.0	...
1396	3119	1.29	≤ -4.00	42.8	...
1397	...	1.60	-0.01	1.0	...
1398	823	0.69	≤ -4.00	80.1	0.0
1400	819	0.73	-2.66	4.5	1.3
1403	824	18.43	-0.24	1.0	-13.4
1404	821	3.51	≤ -4.00	6.9	0.0
1407	825	-0.10	-2.41	2.2	-1.1
1408	5035	0.96	≤ -4.00	13.8	...
1409	826	11.03	≤ -4.00	38.6	-6.3
1410	827	1.07	≤ -4.00	211.6	0.0
1411	828	2.01	≤ -4.00	20.8	0.0
1412	830	4.54	≤ -4.00	3.3	1.8
1413	829	2.51	≤ -4.00	2.0	0.0
1415	831	-0.37	≤ -4.00	1.8	...
1419	834	15.59	≤ -4.00	110.0	...
1421	836	27.27	≤ -4.00	16.6	0.9
1422	10672	0.20	-0.04	1.0	...
1423	838	1.69	≤ -4.00	10.9	0.0
1424	837	6.89	≤ -4.00	3.4	1.2
1425	3042	1.47	≤ -4.00	2.2	...

Table 1—Continued

COUP	Opt. ^a	J^b	$\log P_{\text{KS}}^c$	BB ^d	Ca II ^e
1426	3097	1.05	−3.05	4.7	...
1429	839	6.17	≤ -4.00	4.2	1.2
1431	3129	2.44	−3.52	6.1	...
1432	843	0.02	≤ -4.00	4.8	0.0
1433	3019	3.23	≤ -4.00	86.4	...
1434	845	0.91	≤ -4.00	1.9	−12.2
1435	844	7.96	−1.11	1.0	1.3
1438	848	2.20	≤ -4.00	7.9	2.1
1440	849	0.56	−1.49	1.6	0.9
1443	852	3.11	≤ -4.00	63.2	...
1444	850	27.83	≤ -4.00	96.7	−4.1
1445	855	7.18	−1.93	3.2	0.0
1447	857	−0.07	−2.96	22.0	−4.2
1448	860	6.52	≤ -4.00	2.8	2.1
1449	854	8.90	≤ -4.00	78.0	...
1450	10680	0.49	−3.15	1.3	...
1451	859	1.21	≤ -4.00	9.8	−2.6
1454	863	13.82	≤ -4.00	2.8	0.0
1455	861	0.30	≤ -4.00	79.2	...
1456	3061	1.06	≤ -4.00	51.9	...
1457	3092	2.44	−1.17	1.0	...
1458	865	0.04	−0.67	1.0	1.5
1459	862	0.88	−0.58	1.0	−4.5
1462	866	0.55	≤ -4.00	257.8	...
1463	867	8.16	≤ -4.00	10.6	...
1464	5071	−0.06	≤ -4.00	22.8	...
1466	868	7.74	≤ -4.00	22.8	1.4
1470	5126	0.20	−2.77	1.0	...
1473	2085	0.06	≤ -4.00	11.7	...
1474	872	1.95	≤ -4.00	33.8	0.4
1475	870	2.61	−2.57	3.8	...
1477	10689	0.62	−1.12	1.0	...
1478	871	2.18	≤ -4.00	15.3	...
1479	878	2.38	≤ -4.00	6.9	0.0
1481	880	2.08	≤ -4.00	15.2	0.0
1483	5156	1.38	−0.40	1.0	...
1484	877	0.17	≤ -4.00	12.3	...
1485	879	3.96	≤ -4.00	52.0	−1.4
1487	883	1.45	≤ -4.00	67.5	...
1489	887	−0.94	≤ -4.00	15.9	...
1490	3014	0.28	−2.42	1.5	...
1492	890	1.39	≤ -4.00	10.3	1.6
1495	891	−0.07	−2.68	6.6	0.0
1497	5060	0.41	−1.60	1.0	...
1499	895	45.45	≤ -4.00	283.7	...
1500	892	3.85	≤ -4.00	106.2	1.0
1501	894	0.71	≤ -4.00	9.4	...
1503	5076	0.64	≤ -4.00	31.3	0.0
1507	898	−0.25	≤ -4.00	17.3	0.0
1508	897	0.98	−0.84	1.0	...
1511	901	1.01	≤ -4.00	10.6	...
1512	902	1.25	≤ -4.00	9.4	...
1514	905	0.40	−1.43	1.0	...
1516	907	5.77	≤ -4.00	9.1	1.8
1520	910	0.00	−0.35	1.0	1.8

Table 1—Continued

COUP	Opt. ^a	J^b	$\log P_{\text{KS}}^c$	BB ^d	Ca II ^e
1521	911	16.86	≤ -4.00	4.0	...
1522	912	1.71	-0.44	1.7	1.2
1523	5085	0.69	-0.35	1.0	...
1524	916	0.04	-2.57	1.0	...
1529	5083	1.17	≤ -4.00	7.9	...
1531	3049	1.01	≤ -4.00	1.7	...
1532	5067	-0.55	-0.60	1.0	...
1537	928	-0.04	-0.84	1.0	...
1539	930	0.58	≤ -4.00	8.9	5.2
1540	929	-0.64	-0.42	1.0	0.0
1542	10723	0.16	-2.74	1.0	...
1543	933	-0.13	≤ -4.00	6.5	1.0
1544	931	0.45	≤ -4.00	11.9	2.0
1546	936	1.49	-2.96	22.1	0.8
1547	939	0.42	-1.99	1.0	2.1
1549	942	-0.03	≤ -4.00	17.5	0.0
1550	941	-0.51	≤ -4.00	7.6	1.6
1553	944	2.76	≤ -4.00	31.8	1.2
1558	950	0.13	-0.67	1.0	...
1560	10744	2.63	≤ -4.00	18.9	...
1563	951	6.16	-0.39	1.0	-3.2
1564	954	9.83	-3.70	1.0	0.0
1568	959	0.01	≤ -4.00	90.0	...
1569	958	0.55	-3.70	2.8	-0.4
1570	962	17.22	≤ -4.00	51.9	1.8
1571	965	0.25	≤ -4.00	6.4	0.0
1572	964	1.55	≤ -4.00	3.5	0.0
1573	3107	0.87	-1.74	1.0	...
1576	969	19.22	-0.05	1.0	-2.7
1585	980	23.78	≤ -4.00	2.1	0.0
1588	10776	0.86	-1.70	6.2	...
1590	982	37.01	≤ -4.00	3.8	-1.2
1591	981	1.81	≤ -4.00	15.1	1.7
1592	984	0.86	≤ -4.00	17.5	0.7
1594	990	0.49	≤ -4.00	35.6	0.6
1595	998	5.74	≤ -4.00	6.0	...
1599	1013	1.18	-3.70	4.2	-26.5
1603	5097	0.92	≤ -4.00	21.9	0.0
1604	10817	16.31	-0.47	1.0	...
1608	1026a	26.17	≤ -4.00	35.8	-1.3
1610	1030	4.82	-2.03	1.0	1.5
1611	1032	1.26	-0.05	1.0	0.0
1612	1034	0.38	≤ -4.00	7.7	0.4
1613	1037	1.35	-0.25	1.0	2.5

^aOptical identification from Getman et al. (2005).

^bValue of J statistic; see §2.1.2.

^cKS test probability of X-ray variability; see §2.1.1. Values below -4.00 have been truncated (Getman et al. 2005).

^dRatio of maximum/minimum X-ray flux from BB analysis; see §2.1.1.

^eEquivalent width in Å of the Ca II IR triplet lines. Negative values indicate emission. See Hillenbrand et al. (1998).

Note. — This table is available in its entirety in the

electronic version of the Journal. A portion is shown here for guidance regarding its form and content.

Table 2. Contingency table of optical and X-ray variability in the study sample

Optical variability	X-ray variability	
	Yes	No
Entire study sample ($N = 814$)		
Yes	278	80
No	278	178
Actively accreting stars ($N = 151$)		
Yes	60	25
No	39	27
Non-accreting stars ($N = 145$)		
Yes	64	8
No	59	14

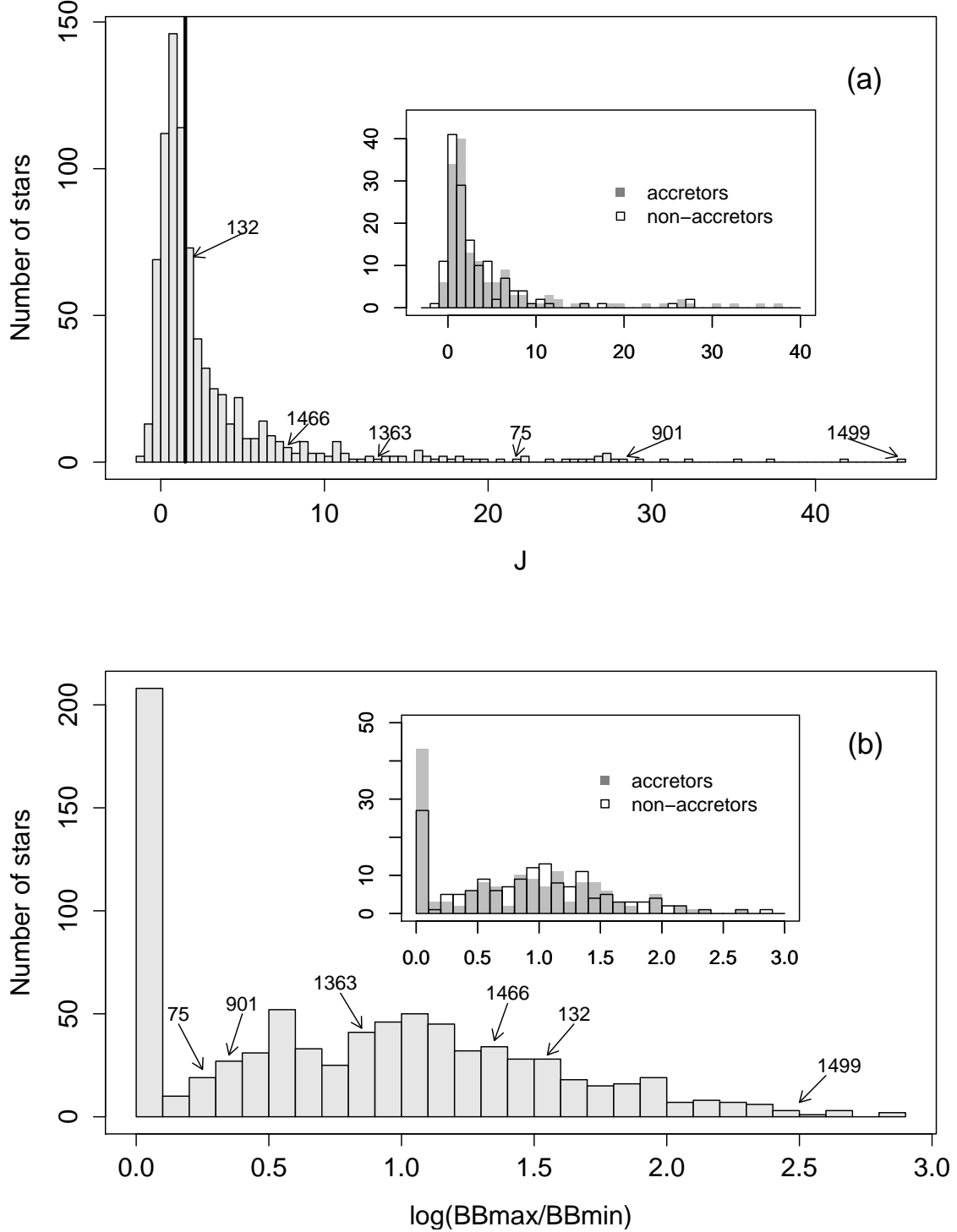


Fig. 1.— (a) Histogram of the J statistic for all stars in the study sample. Chance correlations in the light curves produce a distribution of positive and negative J values centered on zero. The most negative value of J is -1.50 ; thus $J > 1.50$ (indicated by the vertical line) serves as a conservative threshold for identifying stars that are likely true variables. Stars with various values of J above this threshold are indicated; their light curves can be found in Paper I. Inset panel compares the distribution of J separately for accretors and non-accretors as defined in §2. (b) Same as above but for $\log \text{BB}_{\text{max}}/\text{BB}_{\text{min}}$. The first bin is dominated by stars with $\log \text{BB}_{\text{max}}/\text{BB}_{\text{min}} = 0$, which are non-variable in X-rays.

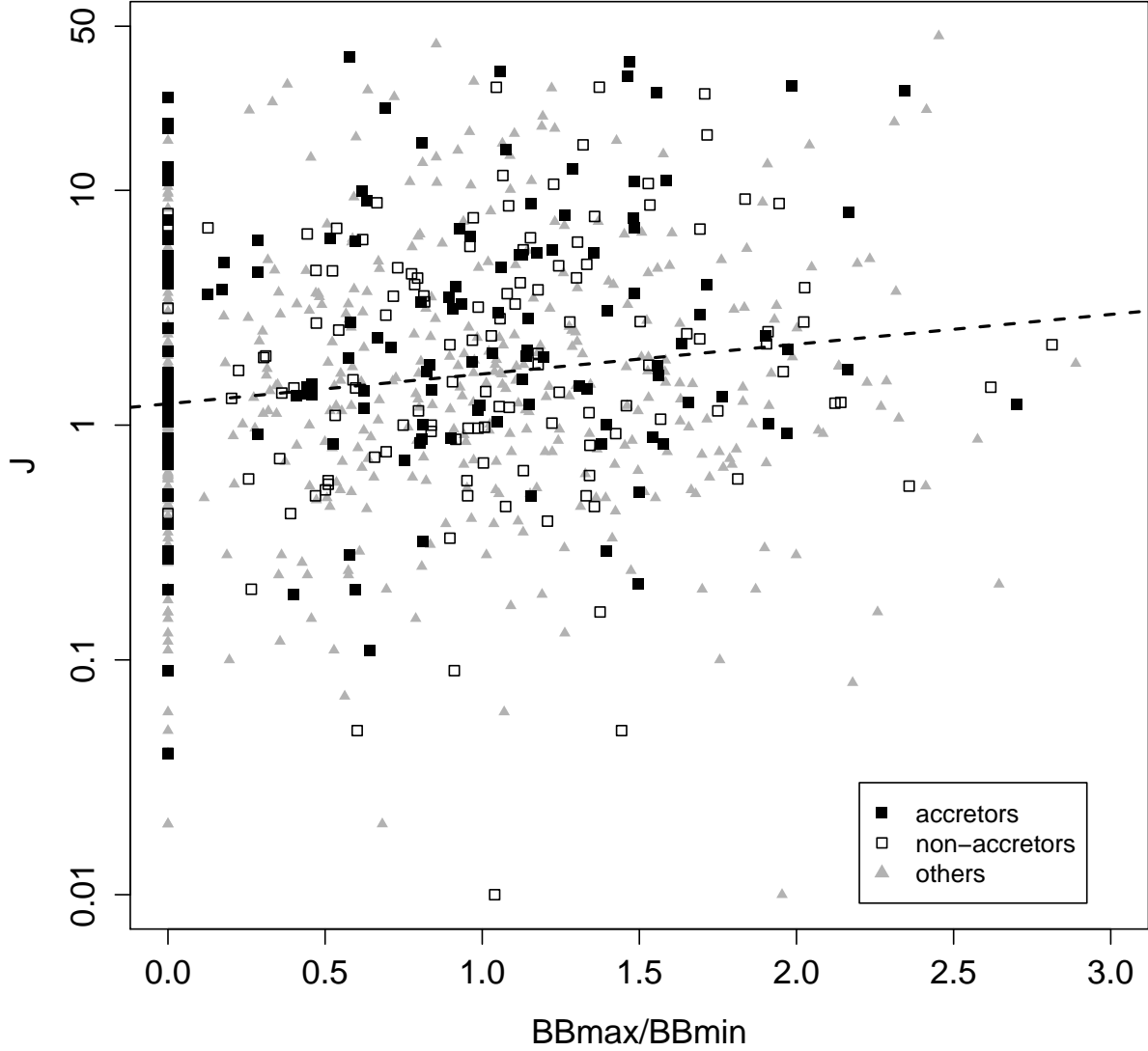


Fig. 2.— Strength of optical variability as measured by the J statistic is plotted vs. strength of X-ray variability as measured by the BB analysis. Stars with negative J have been excluded from the plot so that it may be displayed on a logarithmic scale (see Fig. 1a for explanation of negative J values). The dashed line shows a linear regression fit to all of the data. A statistically significant correlation in the sense of the line is confirmed by a Kendall's τ test. This correlation is found to be the result of the mutual correlation of J and BB_{\max}/BB_{\min} with X-ray luminosity; see text.

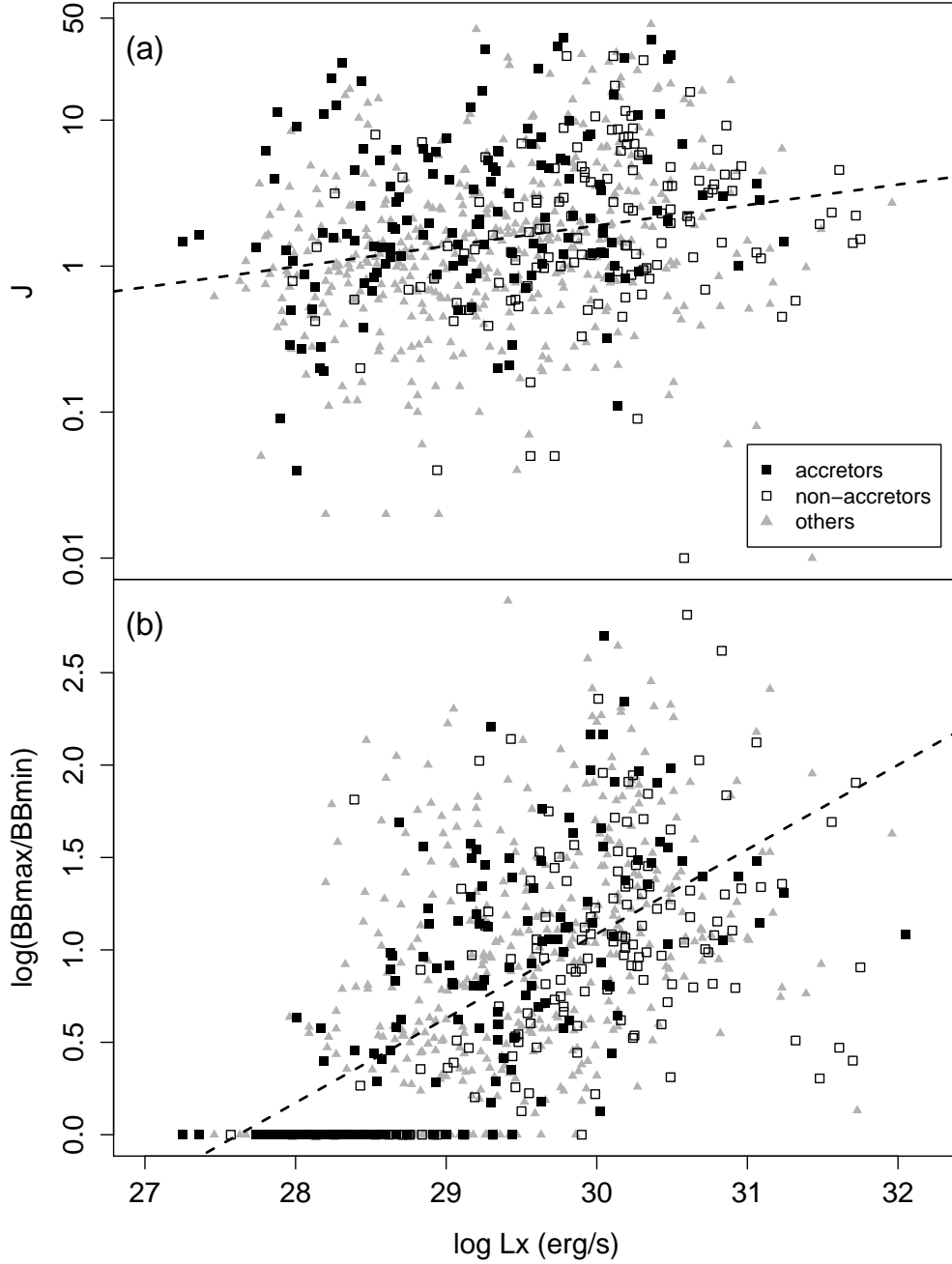


Fig. 3.— (a) Strength of optical variability as measured by the J statistic is plotted vs. X-ray luminosity (L_X). (b) Strength of X-ray variability as measured by the BB analysis is plotted vs. L_X . Symbols and lines are as in Fig. 2. In both panels, a statistically significant correlation in the sense of the line is confirmed by a Kendall's τ test. This correlation is in the same sense when the accretors or non-accretors are tested separately. Only the correlation in (a) is likely to be physical; see text.